

**CHAPTER V**  
**ETHYLENE EPOXIDATION IN CYLINDRICAL**  
**DIELECTRIC BARRIER DISCHARGE:**  
**EFFECTS OF SEPARATE ETHYLENE/OXYGEN FEED**  
(Published in Plasma Chemistry and Plasma Processing (2012))

### **5.1 Abstract**

The effects of separate C<sub>2</sub>H<sub>4</sub>/O<sub>2</sub> feed and C<sub>2</sub>H<sub>4</sub> feed position on the ethylene epoxidation reaction in an AC cylindrical dielectric barrier discharge reactor were investigated. The highest EO selectivity of 34% and EO yield of 7.5%, as well as the lowest power consumption of  $1.72 \times 10^{-16}$  Ws/molecule of EO produced, were obtained at a C<sub>2</sub>H<sub>4</sub> feed position of 0.25, an O<sub>2</sub>/C<sub>2</sub>H<sub>4</sub> feed molar ratio of 1/4, an applied voltage of 13 kV, an input frequency of 550 Hz, and a total feed flow rate of 75 cm<sup>3</sup>/min. The results demonstrated, for the first time, that the separate feed of C<sub>2</sub>H<sub>4</sub> and O<sub>2</sub> could provide better ethylene epoxidation performance in terms of higher EO selectivity and yield, and lower power consumption, as compared to the mixed feed. All undesired reactions including C<sub>2</sub>H<sub>4</sub> cracking, dehydrogenation, oxidation, and coupling reactions are lowered by the ethylene separate feed because of a decrease in opportunity of ethylene molecules to be activated by generated electrons.

**Keywords:** Epoxidation; Ethylene oxide; Dielectric barrier discharge; Feed position

### **5.2 Introduction**

Ethylene epoxidation, the selective oxidation of ethylene, is an important reaction in the petrochemical industry because ethylene oxide (C<sub>2</sub>H<sub>4</sub>O, EO) can be produced commercially by the partial oxidation with high selectivity over silver (Ag)-based catalysts as discovered by Lefort [1]. Ethylene oxide is used as a key feedstock or intermediate for the production of various useful chemicals such as

surfactants, polyesters, antifreezes, automotive coolants, solvents, and adhesives. Besides, it is also used in the production of a sterilant for foodstuffs. Therefore, this epoxidation reaction has been investigated extensively.

Commercially, the conventional catalytic process for ethylene epoxidation uses low-surface-area  $\alpha$ -alumina-supported silver catalysts (Ag/(LSA)  $\alpha$ -Al<sub>2</sub>O<sub>3</sub>). Although these commercial catalysts provide quite high EO selectivity, the ethylene and oxygen conversions are still very low (1-2%); therefore, many studies have endeavored to develop more effective Ag catalysts for enhancing EO production. Several studies indicate that alkali and transition noble metals, especially Cs, Cu, Re, and Au, as well as halogen promoters such as Cl, can provide improved EO selectivity [2-15]. However, the currently-used catalytic process still requires high temperatures for efficient operation, resulting in high energy consumption. In addition, catalyst deactivation results from both coke formation and sintering of active sites on the catalyst surface commonly occurs at high temperatures, leading to decreases in both catalytic activity and desired product selectivity. Hence, development of new techniques for solving these mentioned problems and enhancing the ethylene epoxidation activity are of great interest.

Non-thermal plasma is a promising technique for many potential applications, such as surface modification [16], chemical synthesis [15,17-19], hydrocarbon reforming [20-25], and gas treatment [26-29]. An interesting characteristic of the non-thermal plasma is that the bulk gas temperature is still very low (close to ambient temperature) even though generated high energy electrons have a much higher temperature (approximately  $10^4$ - $10^5$  K) [26,30]. As a consequence, the non-thermal plasma can be operated at an ambient temperature and atmospheric pressure, leading to low energy consumption. Hence, catalyst deactivation under high-temperature operation can also be avoided by this technique. The plasma discharges can be generated by applying an electrical current with a sufficient voltage across metal electrodes. Subsequently, the reactant gases passing through the plasma discharge zone are collided with the generated electrons to create various high energetic species, leading to initiation of subsequent chemical reactions.

Because of the mentioned advantages of non-thermal plasma, many research studies have increasingly investigated several chemical reactions by using various

types of non-thermal plasmas, such as dielectric barrier discharges (DBD) [17,24,25,29,35,37-39], corona discharges [15,16,19,28], glow discharges [32], microwave discharges [23], and sliding discharge [22]. The corona discharges, as well as parallel and cylindrical DBD, have been recently investigated for ethylene epoxidation in the presence and absence of silver catalysts [15,34,35,37,38]. Ethylene epoxidation over Ag catalysts was, for first time, investigated in a corona discharge [34], and the effects of promoters, such as Cs, Cu, and Au, were subsequently studied [15]. The ethylene epoxidation activity could be enhanced when appropriate Ag catalysts were applied in a plasma system. Furthermore, the ethylene epoxidation performance under a corona discharge was compared to that under parallel DBD, and the results showed that the parallel DBD provided better performance in terms of higher EO yield and lower power consumption per EO molecule produced [35]. Subsequently, the DBD systems with two different electrode geometries, parallel and cylindrical electrodes, were comparatively investigated for ethylene epoxidation [37]. The cylindrical DBD system exhibited superior epoxidation performance in terms of the high EO selectivity compared to the parallel DBD system. Recently, our group reported that ethylene epoxidation under a parallel DBD was improved by applying a suitable SiO<sub>2</sub>-supported Ag catalyst [38]. For the combined parallel DBD with the Ag catalyst, the EO selectivity significantly increased as compared to the sole cylindrical DBD. However, several undesired reactions including deep oxidation, partial oxidation, cracking, dehydrogenation, and coupling reactions normally occur in plasma environments.

Generally, ethylene (C<sub>2</sub>H<sub>4</sub>), oxygen (O<sub>2</sub>), and helium (He, as a balance gas) are basically fed into a plasma reactor as the mixed feed for ethylene epoxidation reaction. Hence, both C<sub>2</sub>H<sub>4</sub> and O<sub>2</sub> molecules are collided by the energetic electrons to initiate several subsequential chemical reactions including ethylene epoxidation and undesired reactions. It was hypothesized that a separate feed of C<sub>2</sub>H<sub>4</sub> from O<sub>2</sub> with a suitable C<sub>2</sub>H<sub>4</sub> feed position could reduce all the mentioned undesired reactions including cracking, dehydrogenation, coupling, and complete oxidation reactions of C<sub>2</sub>H<sub>4</sub>, resulting in a higher EO selectivity and lower by-product selectivities. To our knowledge, the effect of separate C<sub>2</sub>H<sub>4</sub>/O<sub>2</sub> feed on the ethylene epoxidation performance using a cylindrical DBD system has never been investigated before.

Therefore, this present work focused, for the first time, on optimizing the C<sub>2</sub>H<sub>4</sub> feed position in a cylindrical DBD system to improve the ethylene epoxidation performance. Under the separate C<sub>2</sub>H<sub>4</sub>/O<sub>2</sub> feed condition, various operational parameters, including O<sub>2</sub>/C<sub>2</sub>H<sub>4</sub> feed molar ratio, applied voltage, input frequency, and total feed flow rate, were also investigated to obtain the best conditions for EO production. The ethylene epoxidation performance of the separate C<sub>2</sub>H<sub>4</sub>/O<sub>2</sub> feed was compared to that of the mixed C<sub>2</sub>H<sub>4</sub>/O<sub>2</sub> feed under their own optimum conditions.

### 5.3 Experimental

#### 5.3.1 Reactant Gases

Gases used in this work were 99.995% helium (high purity grade), 40% ethylene in helium ( $\pm 1\%$  uncertainty), and 97% oxygen in helium ( $\pm 1\%$  uncertainty). The 30% ethylene oxide in helium ( $\pm 1\%$  uncertainty) was used as a standard gas to obtain the calibration curve of gas chromatography (GC) for EO analysis. All gases were specially blended by Thai Industrial Gas Co., Ltd.

#### 5.3.2 Experimental Setup and Reaction Activity Experiments

The ethylene epoxidation reaction was investigated in a cylindrical dielectric barrier discharge reactor at ambient temperature (25–27°C) and atmospheric pressure. The schematic of the experimental setup is shown in Figure 5.1(a). The reactor consisted of two electrode tubes made of stainless steel. The outer electrode had a 1.5 cm inner diameter (ID), a 1.9 cm outer diameter (OD), and a 16 cm height whereas the inner electrode had a 0.5 cm OD and 14 cm height. For the adjustment of the C<sub>2</sub>H<sub>4</sub> feed position, stainless steel tubes with a 0.3 cm OD were connected to the outside of the outer electrode at 5 equally-spaced positions on the electrode in a range from 0 (at the inlet of outer electrode) to 1 (at the outlet of outer electrode), as shown in Figure 5.1(b).

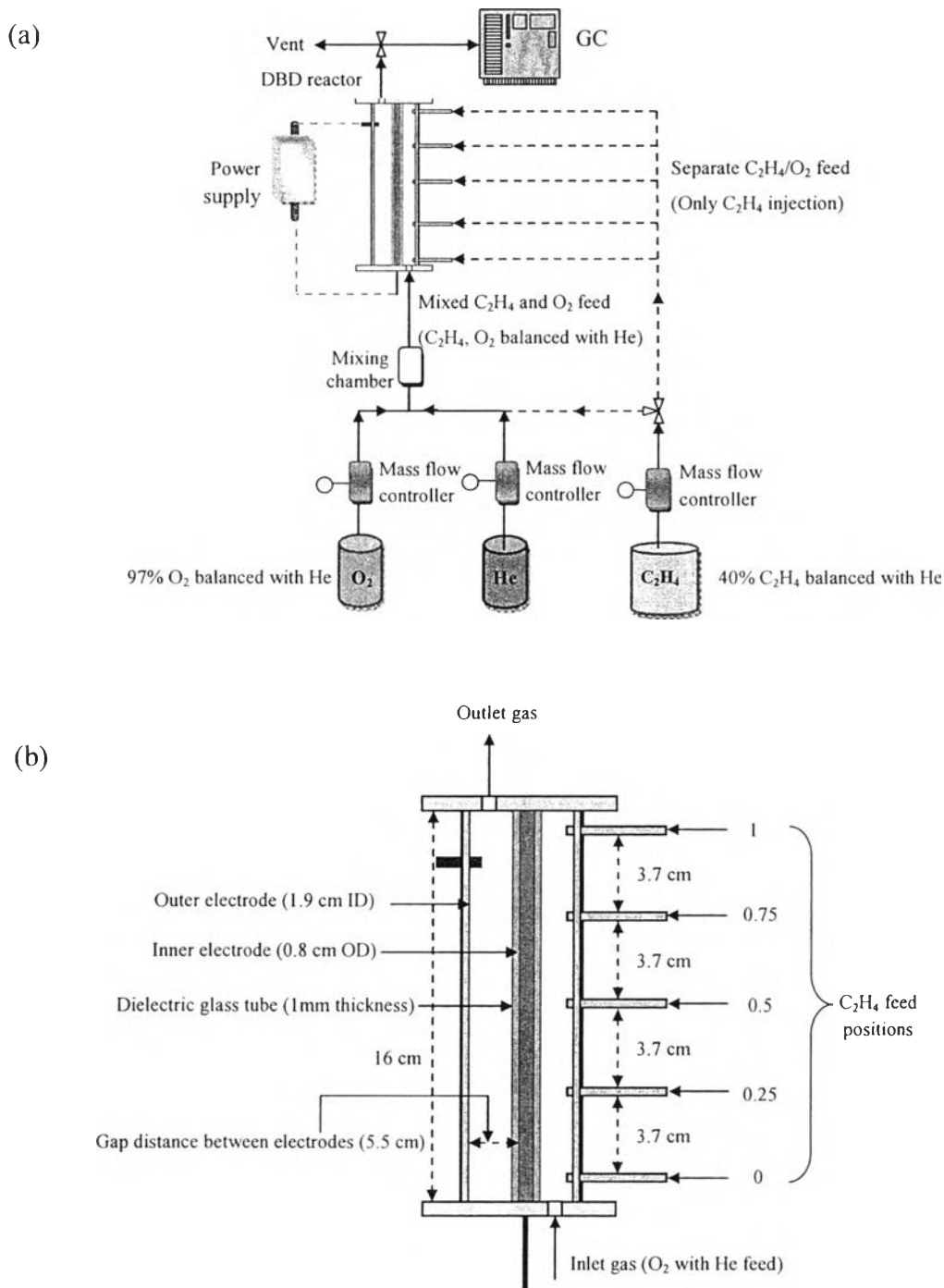


**Figure 5.1** (a) Schematic of experimental setup of DBD plasma system for the ethylene epoxidation reaction and (b) the configuration of the cylindrical DBD reactor.

A dielectric glass tube with a 1 mm thickness was placed on the outer surface of the inner electrode, between two concentric electrodes. The gap distance between the two electrodes was fixed at 0.5 cm and the studied DBD reactor had a working volume of 22 cm<sup>3</sup>. There were three steps to convert the domestic AC input

to a high-voltage AC output. First, the domestic AC input power of 220 V and 50 Hz was transformed to the DC output of 70 V by a DC power supply converter. Next, a 500 W power amplifier with a function generator was employed for converting the DC to the AC with a sinusoidal waveform and different frequencies. The outlet voltage was subsequently stepped up by using a high-voltage transformer. Finally, high-voltage AC was produced, and its output voltage and frequency were varied by the function generator, whereas its sinusoidal wave signal was monitored by an oscilloscope. The description of the power supply system and electrical measurements were given elsewhere [33]. Thus, the low-side voltage, input power, and current were measured by a power analyzer (Extech Instruments Corporation, True RMS Single Phase Power Analyzer, 380801). The high-side voltage and current were computed by multiplying and dividing the measured values by a factor of 130, respectively, since they were not able to be measured precisely across the electrodes (high-voltage side) because of its non-equilibrium in nature.

For the epoxidation reaction activity experiments, ethylene ( $C_2H_4$ ), oxygen ( $O_2$ ), and helium (He, as a balance gas)—controlled by electronic mass flow controllers—were fed into a cylindrical DBD system. The studied DBD system was operated under the base conditions: an  $O_2/C_2H_4$  feed molar ratio of 1/4, an electrode gap distance of 0.5 cm, an input frequency of 500 Hz, and an applied voltage of 15 kV, which were the optimum conditions (for a cylindrical DBD system with the mixed feed) obtained from our previous work [37], while the total feed flow rate was initially fixed at  $75\text{ cm}^3/\text{min}$  and the  $C_2H_4$  feed position was varied in order to investigate the effect of separate  $C_2H_4/O_2$  feed on the ethylene epoxidation activity, and to obtain the optimum  $C_2H_4$  feed position for maximum EO production performance. After obtaining the optimum  $C_2H_4$  feed position, the effects of the feed molar ratio of  $O_2$ -to- $C_2H_4$ , applied voltage, input frequency, and total feed flow rate were examined. Table 5.1 shows the flow rates of the three gas streams ( $C_2H_4$ ,  $O_2$ , and He) for each total flow rate used in this study to investigate the effect of total feed flow rate. Finally, the ethylene epoxidation performance of the separate  $C_2H_4/O_2$  feed was compared to that of the mixed  $C_2H_4/O_2$  feed. All reactant lines had a  $0.7\text{ }\mu\text{m}$  in-line filter to entrap any solid particles before flowing through the mass flow controllers. After compositions of the outlet gas became invariant with time, the

**Table 5.1** Flow rates of three feed gases for each total feed flow rate used in this study

| <b>Flow rate (cm<sup>3</sup>/min)</b> |                          |               |                   |
|---------------------------------------|--------------------------|---------------|-------------------|
| <b>40% C<sub>2</sub>H<sub>4</sub></b> | <b>97% O<sub>2</sub></b> | <b>Helium</b> | <b>Total feed</b> |
| 24                                    | 2.4                      | 33.6          | 60                |
| 30                                    | 3                        | 42            | 75                |
| 40                                    | 4                        | 56            | 100               |
| 50                                    | 5                        | 70            | 125               |

power supply was turned on to create a discharge. The product gas was allowed to pass through a water trap filter before flowing to an on-line GC for analysis every 20 min. The on-line GC (PerkinElmer, AutoSystem GC), equipped with both a thermal conductivity detector (TCD) and a flame ionization detector (FID), was used to analyze the compositions of both reactant and product gases. For the TCD channel, a packed column (Carboxen 1000) was used for the analysis of hydrogen (H<sub>2</sub>), oxygen (O<sub>2</sub>), carbon monoxide (CO), and carbon dioxide (CO<sub>2</sub>). For the FID channel, a capillary column (OV-Plot U) was used for EO and other hydrocarbon product analyses. For any studied conditions, the system was operated to reach steady state before taking outlet gas samples. At least 5 outlet gas samples were taken for analysis of gas composition using the online GC. To ensure reproducibility of the experimental data, the experiments were repeated for 3 times. All experimental data were averaged with a standard deviation of less than 5% and the average data were used to assess the process performance of the studied DBD system. Then, the experiment data were used to calculate the C<sub>2</sub>H<sub>4</sub> and O<sub>2</sub> conversions, the product selectivities, including H<sub>2</sub>, CO, CO<sub>2</sub>, EO, CH<sub>4</sub>, C<sub>2</sub>H<sub>6</sub>, C<sub>2</sub>H<sub>2</sub>, and traces of C<sub>3</sub>, and the EO yield. These calculations were used for evaluating the process performance and are defined as follows:

$$\% \text{ Reactant conversion} = \frac{(\text{moles of reactant in} - \text{moles of reactant out}) \times 100}{(\text{moles of reactant in})} \quad (5.1)$$

$$\% \text{ Product selectivity} = \frac{\text{moles of product produced} \times 100}{\text{total moles of products produced}} \quad (5.2)$$

$$\% \text{ EO yield} = \frac{(\% \text{ C}_2\text{H}_4 \text{ conversion}) \times (\% \text{ EO selectivity})}{100} \quad (5.3)$$

In addition, power consumption was calculated in a unit of Ws per C<sub>2</sub>H<sub>4</sub> molecule converted or per EO molecule produced using the following equation:

$$\text{Power consumption} = \frac{P \times 60}{N \times M} \quad (5.4)$$

where P = Power (W)

N = Avogadro's number =  $6.02 \times 10^{23}$  molecules/mol

M = Rate of converted C<sub>2</sub>H<sub>4</sub> molecules in feed or rate of produced EO molecules (mol/min).

## 5.4 Results and Discussion

### 5.4.1 Possible Chemical Reactions in the Studied DBD System

To obtain a better understanding of chemical pathways for ethylene epoxidation and other reactions under the studied conditions, all possible chemical pathways that may appear in the cylindrical DBD system are proposed in the following equations [40-45]:

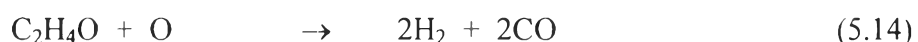
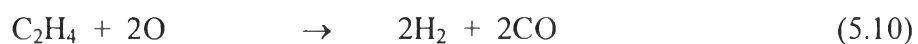
Active oxygen formation:



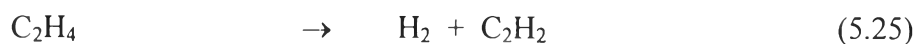
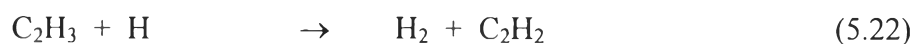
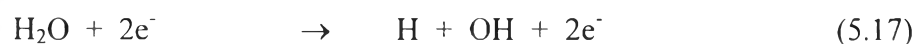
Ethylene epoxidation:



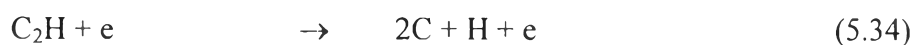
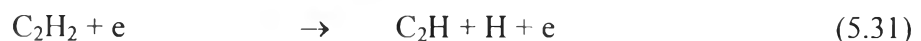
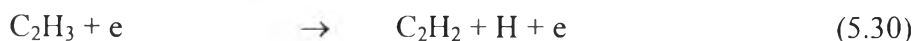
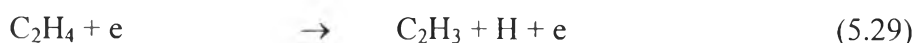
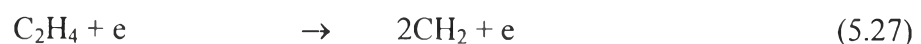
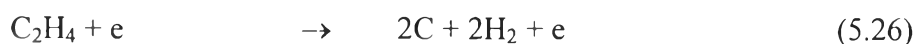
Combustion or deep oxidation:



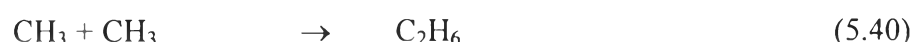
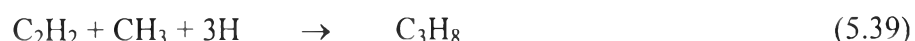
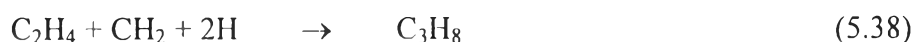
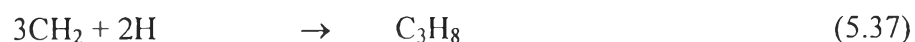
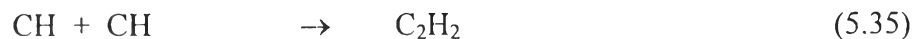
Dehydrogenation or Acetylene formation:



Cracking:



Coupling:



#### 5.4.2 Effect of Ethylene Feed Position

The effect of the  $\text{C}_2\text{H}_4$  feed position in the cylindrical DBD system was initially investigated for the ethylene epoxidation reaction. The  $\text{C}_2\text{H}_4$  and  $\text{O}_2$  conversions, product selectivities and concentrations, EO yield, and power consumption in the relation to the  $\text{C}_2\text{H}_4$  feed position are shown in Figure 5.2. From the results, the  $\text{C}_2\text{H}_4$  feed position greatly influenced the  $\text{O}_2$  conversion but only slightly affected the  $\text{C}_2\text{H}_4$  conversion (Figure 5.2(a)). The  $\text{O}_2$  conversion significantly decreased with increasing  $\text{C}_2\text{H}_4$  feed position from 0 to 1. These results can be explained by the fact that an increase in the  $\text{C}_2\text{H}_4$  feed position from 0 to 1 results in a decrease in reaction time between the  $\text{O}_2$  and  $\text{C}_2\text{H}_4$ , as well as a decrease in opportunity for the  $\text{C}_2\text{H}_4$  molecules to be activated by the generated electrons to form various active species. Therefore, the  $\text{O}_2$  conversion decreased with increasing  $\text{C}_2\text{H}_4$  feed position up to 1. In addition, when comparing the  $\text{C}_2\text{H}_4$  and  $\text{O}_2$  conversions, it was clearly observed that the  $\text{O}_2$  conversion was much higher than the  $\text{C}_2\text{H}_4$  conversion over the entire studied range of  $\text{C}_2\text{H}_4$  feed positions. This is possible because 1 mole of  $\text{C}_2\text{H}_4$  requires 1/2, 2, and 3 moles of  $\text{O}_2$  for the formation of EO, CO, and  $\text{CO}_2$ , respectively. Interestingly, the EO yield exhibits a similar trend as the  $\text{O}_2$  conversion. The EO yield rapidly decreased with increasing  $\text{C}_2\text{H}_4$  feed position up to 0.75, and there was no EO production at the  $\text{C}_2\text{H}_4$  feed position range from 0.75 to 1 (Figure 5.2(a)).

As shown in Figure 5.2(b), the EO selectivity slightly increases with increasing  $\text{C}_2\text{H}_4$  feed position from 0 to 0.5, and reaches a maximum at the  $\text{C}_2\text{H}_4$  feed position of 0.5. When the  $\text{C}_2\text{H}_4$  feed position increased from 0.5 to 0.75 and 1, the EO selectivity became zero. The  $\text{H}_2$  and  $\text{C}_2\text{H}_2$  selectivities decreased with increasing

$C_2H_4$  feed position up to 1, whereas only traces of  $CO_2$ ,  $CH_4$ ,  $C_2H_6$ , and  $C_3H_8$  (lower than 3%) were produced over the entire  $C_2H_4$  feed position range. It is interesting to point out that  $C_3H_8$  was the largest hydrocarbon with a small fraction produced under the studied conditions. In addition, it was observed that only the CO selectivity greatly increased with increasing  $C_2H_4$  feed position from 0 to 1.

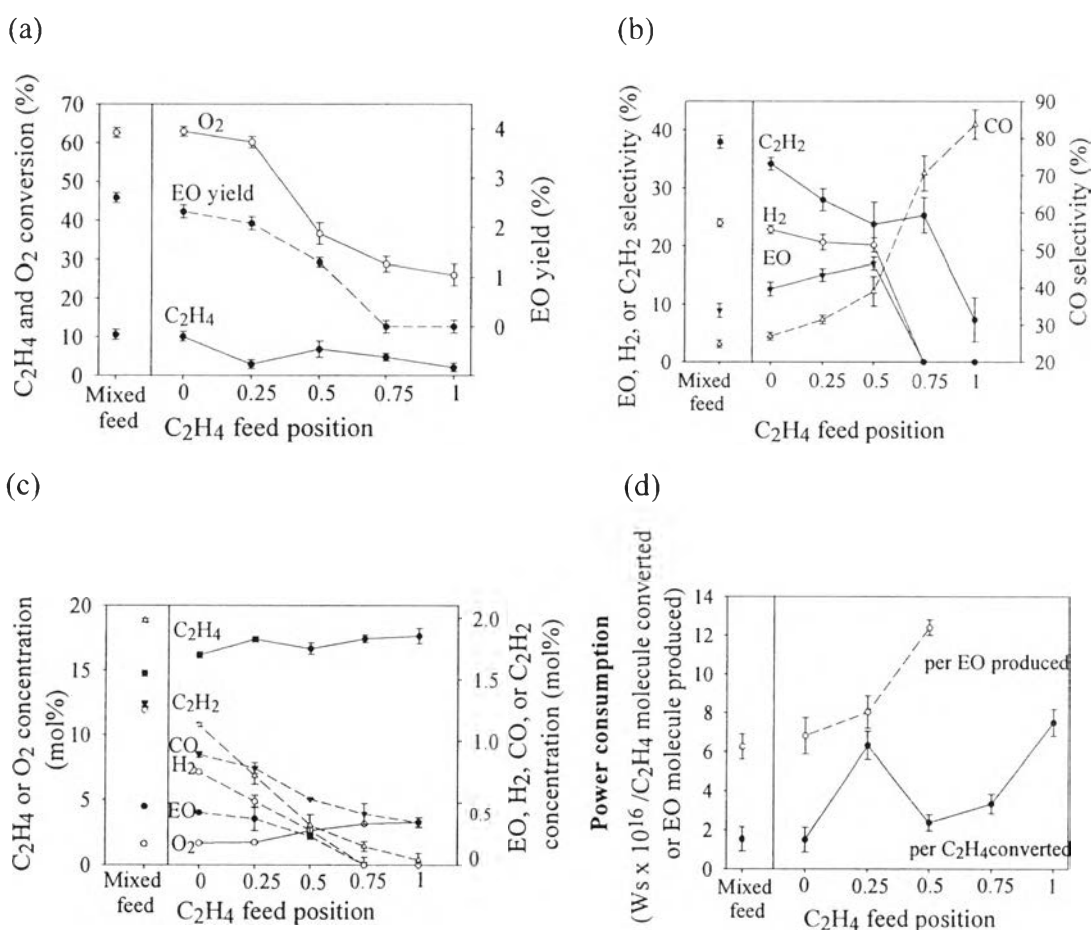


**Figure 5.2** (a)  $C_2H_4$  and  $O_2$  conversions and EO yield, (b) product selectivities, (c) outlet gas concentrations, and (d) power consumption as a function of  $C_2H_4$  feed position (a  $O_2/C_2H_4$  feed molar ratio of 1/4, an applied voltage of 15 kV, an input frequency of 500 Hz, and a total feed flow rate of  $75 \text{ cm}^3/\text{min}$ ) as compared with the mixed feed.

Figure 5.2(c) shows the concentrations of outlet gas stream, including  $C_2H_4$  and  $O_2$  residual reactants, EO, and other main products ( $H_2$ ,  $CO$ , and  $C_2H_2$ ) as a

function of the  $C_2H_4$  feed position, whereas the concentrations of other by-products, i.e.  $CO_2$ ,  $CH_4$ , and  $C_3H_8$ , are not shown here because of their extremely low concentrations (lower than 0.1 mol%). The results suggest that under the lean oxygen condition with a short resident time for the feed  $C_2H_4$ , only three dominant reactions of CO formation, ethylene epoxidation, and dehydrogenation can occur in the studied DBD system. The EO and all other main product concentrations markedly decreased with increasing  $C_2H_4$  feed position from 0 to 1, whereas the  $C_2H_4$  concentration remained almost unchanged and the  $O_2$  concentration increased. The decreases in all product concentrations with increasing  $C_2H_4$  feed position are due to the reduction of  $C_2H_4$  residence time.

Figure 5.2(d) shows the power consumption as a function of the  $C_2H_4$  feed position. The power consumption per EO molecule produced increased with increasing  $C_2H_4$  feed position up to 0.5. Beyond the  $C_2H_4$  feed position of 0.5, the system could not produce EO; thus, the power consumption per EO molecule produced was not calculated. The power consumption per  $C_2H_4$  molecule converted increased with increasing  $C_2H_4$  feed position and reached a maximum at the  $C_2H_4$  feed position of 0.25, and then decreased with further increasing  $C_2H_4$  feed position from 0.25 to 0.5. After that, it increased again with increasing  $C_2H_4$  feed position from 0.5 to 1.

When comparing the mixed  $C_2H_4/O_2$  feed and the separate  $C_2H_4/O_2$  feed, especially at two  $C_2H_4$  feed positions of 0.25 and 0.5, the separate feed could reduce ethylene cracking, dehydrogenation, and coupling reactions, as shown experimentally by an increase in the EO selectivity and decreases in the  $H_2$  and  $C_2H_2$  selectivities. For the two short  $C_2H_4$  feed positions (0.25 and 0.5), the cylindrical DBD system provided comparatively high  $O_2$  conversion as compared with the other two long  $C_2H_4$  feed positions (0.75 and 1). This is the result of more  $C_2H_4$  molecules being activated by the generated electrons, which were further reacted with the oxygen active species in the system. The high EO yield and selectivity, as well as high selectivities for several other products, were obtained from the cylindrical DBD system with the two short  $C_2H_4$  feed positions. In contrast, with two long  $C_2H_4$  feed positions (0.75 and 1), the  $C_2H_4$  molecules had less of a chance to be activated by the energetic electrons, which led to lower cracking and oxidation reaction rates, as well

as the epoxidation reaction. As a consequence, all the product concentrations and the EO yield decreased. Hence, the system should be operated with a suitable  $C_2H_4$  feed position, which can provide both high EO yield and selectivity with lower selectivities for other products. From all these results, the  $C_2H_4$  feed position of 0.25 was considered to be an optimum value for ethylene epoxidation in the cylindrical DBD system and used in further experiments because it provided comparatively high EO selectivity and EO yield, as well as reasonably low power consumption per EO molecule produced. It is worth whole mentioning that even though the separate  $C_2H_4/O_2$  feed did not show significant enhancement of ethylene epoxidation performance as compared to the mixed  $C_2H_4/O_2$  feed, we hypothesize that the DBD system with the separate  $C_2H_4/O_2$  feed was not yet operated under its own optimum conditions. Hence, next experiments were performed to obtain the optimum conditions of the separate  $C_2H_4/O_2$  feed system for the ethylene epoxidation reaction.

#### 5.4.3 Effect of $O_2/C_2H_4$ Feed Molar Ratio

The  $O_2/C_2H_4$  feed molar ratio was varied in the range of 1/5–1/0.67 to determine its effect on ethylene epoxidation in the cylindrical DBD system. As shown in Figure 5.3(a), the  $C_2H_4$  conversion remains almost unchanged at around 3% with the exception of the  $O_2/C_2H_4$  feed molar ratio of 1/0.67, which provides a slightly higher  $C_2H_4$  conversion of 9%; while the  $O_2$  conversion tends to decrease with increasing  $O_2/C_2H_4$  feed molar ratio. The results indicate that the increasing  $O_2/C_2H_4$  feed molar ratio has more negative influence on the  $O_2$  conversion than on the  $C_2H_4$  conversion. As shown in Figure 5.3(a), the EO yield rapidly increases when the  $O_2/C_2H_4$  feed molar ratio increases from 1/5 to 1/4, and then adversely decreases with further increasing  $O_2/C_2H_4$  feed molar ratio beyond 1/4. Interestingly, the  $O_2/C_2H_4$  feed molar ratio of 1/4 provided the highest EO yield. Beyond the  $O_2/C_2H_4$  feed molar ratio of 1/4, the EO yield greatly decreased with further increasing  $O_2/C_2H_4$  feed molar ratio.

The EO selectivity slightly decreased with increasing  $O_2/C_2H_4$  feed molar ratio while the CO selectivity increased (Figure 5.3(b)). The  $H_2$  selectivity also tended to slightly increase, whereas the  $C_2H_2$  selectivity seemed to fluctuate with an increase in the  $O_2/C_2H_4$  feed molar ratio. The results can be explained by the fact that

the quantity of oxygen free radicals increased when the  $O_2/C_2H_4$  feed molar ratio increased, leading to the promotion of hydrocarbon combustion rather than ethylene epoxidation, as experimentally evidenced by the increase in CO selectivity and concentration and the decrease in EO selectivity and concentration (Figure 5.3(b) and Figure 5.3(c)). The present results confirm that an  $O_2$ -lean condition is basically required to maximize ethylene epoxidation. However, there was a reduction of ethylene epoxidation activity when the system had insufficient available oxygen free radicals, especially at the lowest  $O_2/C_2H_4$  feed molar ratio of 1/5. This resulted in decreased EO yield, as well as lower  $H_2$ , CO, and  $C_2H_2$  selectivities, as compared to those at the  $O_2/C_2H_4$  feed molar ratio of 1/4 (Figure 5.3(a)).

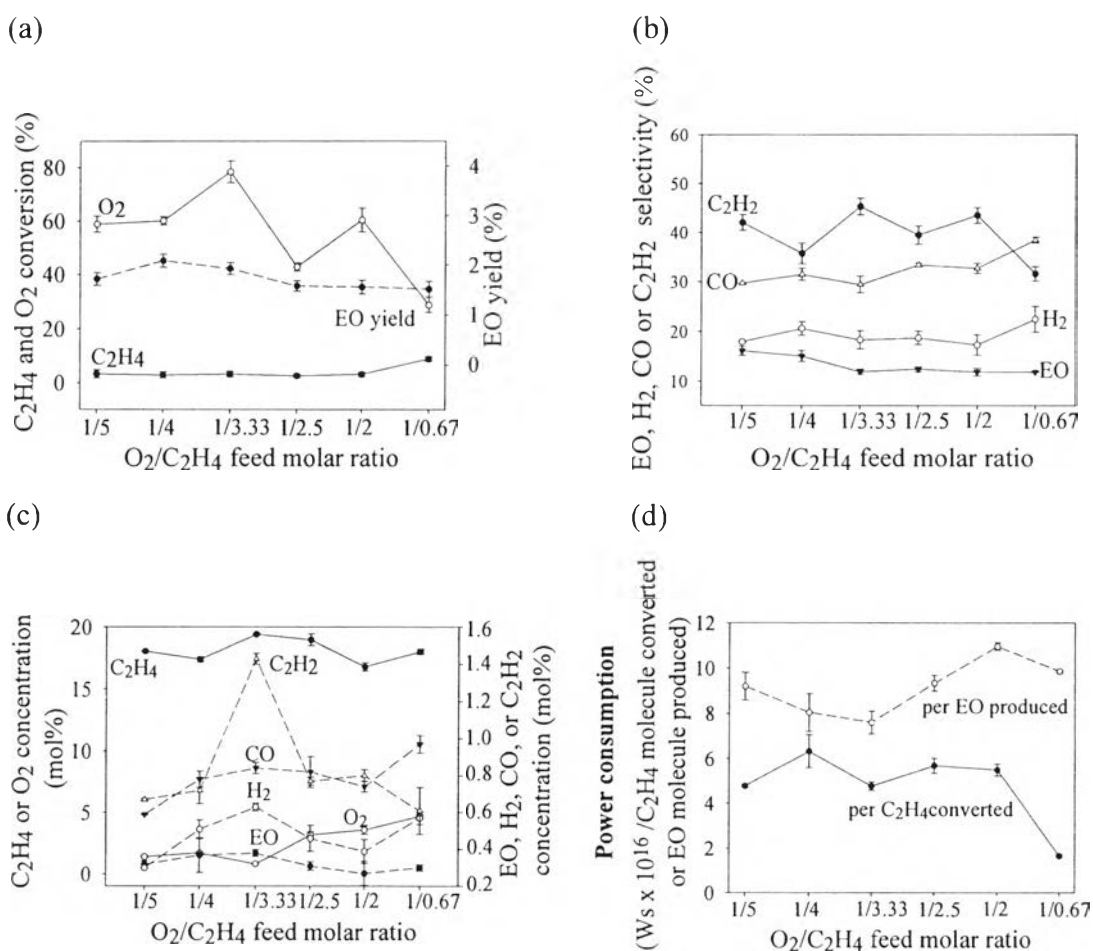


**Figure 5.3** a)  $C_2H_4$  and  $O_2$  conversions and EO yield, (b) product selectivities, (c) outlet gas concentrations, and (d) power consumption as a function of  $O_2/C_2H_4$  feed molar ratio (a  $C_2H_4$  feed position of 0.25, an applied voltage of 15 kV, an input frequency of 500 Hz, and a total feed flow rate of  $75 \text{ cm}^3/\text{min}$ ).

The  $C_2H_4$  concentration was nearly unchanged even though the  $O_2/C_2H_4$  feed molar ratio increased from 1/5 to 1/0.67, while the  $O_2$  concentration tended to increase with increasing  $O_2/C_2H_4$  feed molar ratio, which agreed well with the decrease in the  $O_2$  conversion (Figure 5.3(a) and Figure 5.3(c)). The EO and  $H_2$  concentrations increased with increasing  $O_2/C_2H_4$  feed molar ratio from 1/5 to 1/3.33, and then decreased when the  $O_2/C_2H_4$  feed molar ratio further increased beyond 1/3.33. A maximum  $C_2H_2$  concentration was also found at the  $O_2/C_2H_4$  feed molar ratio of 1/3.33, whereas the CO concentration had the same trend as the CO selectivity, which tended to increase with increasing  $O_2/C_2H_4$  feed molar ratio.

The power consumption per  $C_2H_4$  molecule converted tended to decrease with increasing  $O_2/C_2H_4$  feed molar ratios, whereas the power consumption per EO molecule produced gradually decreased when the  $O_2/C_2H_4$  feed molar ratio increased from 1/5 to 1/3.33, and adversely increased with further increasing  $O_2/C_2H_4$  feed molar ratio beyond 1/3.33 (Figure 5.3(d)). Based on these results, the  $O_2/C_2H_4$  feed molar ratio of 1/4 was found to be an optimum ratio because it provided better ethylene epoxidation performance, exhibiting the highest EO yield, a comparatively high EO selectivity, as well as almost lowest power consumption per EO molecule produced.

#### 5.4.4 Effect of Applied Voltage

The electrical process parameters of applied voltage and input frequency influence the field strength, stability and uniformity of generated discharges. In this study, the input power was varied by adjusting either the applied voltage or input frequency independently. For the investigated cylindrical DBD system, the breakdown voltage, or the lowest voltage required to initiate plasma discharges, was about 12 kV, and uniform and stable plasma discharges could not exist at a voltage above 17 kV. Therefore, the applied voltage was investigated in the range of 12–17 kV. From the results, the  $C_2H_4$  conversion remained almost unchanged with increasing applied voltage, whereas the  $O_2$  conversion was constant, and then drastically decreased with a further increase in applied voltage beyond 14 kV (Figure 5.4(a)). As shown in Figure 5.4(b), the input power slightly increases in the low applied voltage range of 12–14 kV, and then gradually increases with further

increasing applied voltage over 14 kV. Consequently, the generated current increases with increasing applied voltage. However, the results in Figure 5.4(a) did not agree

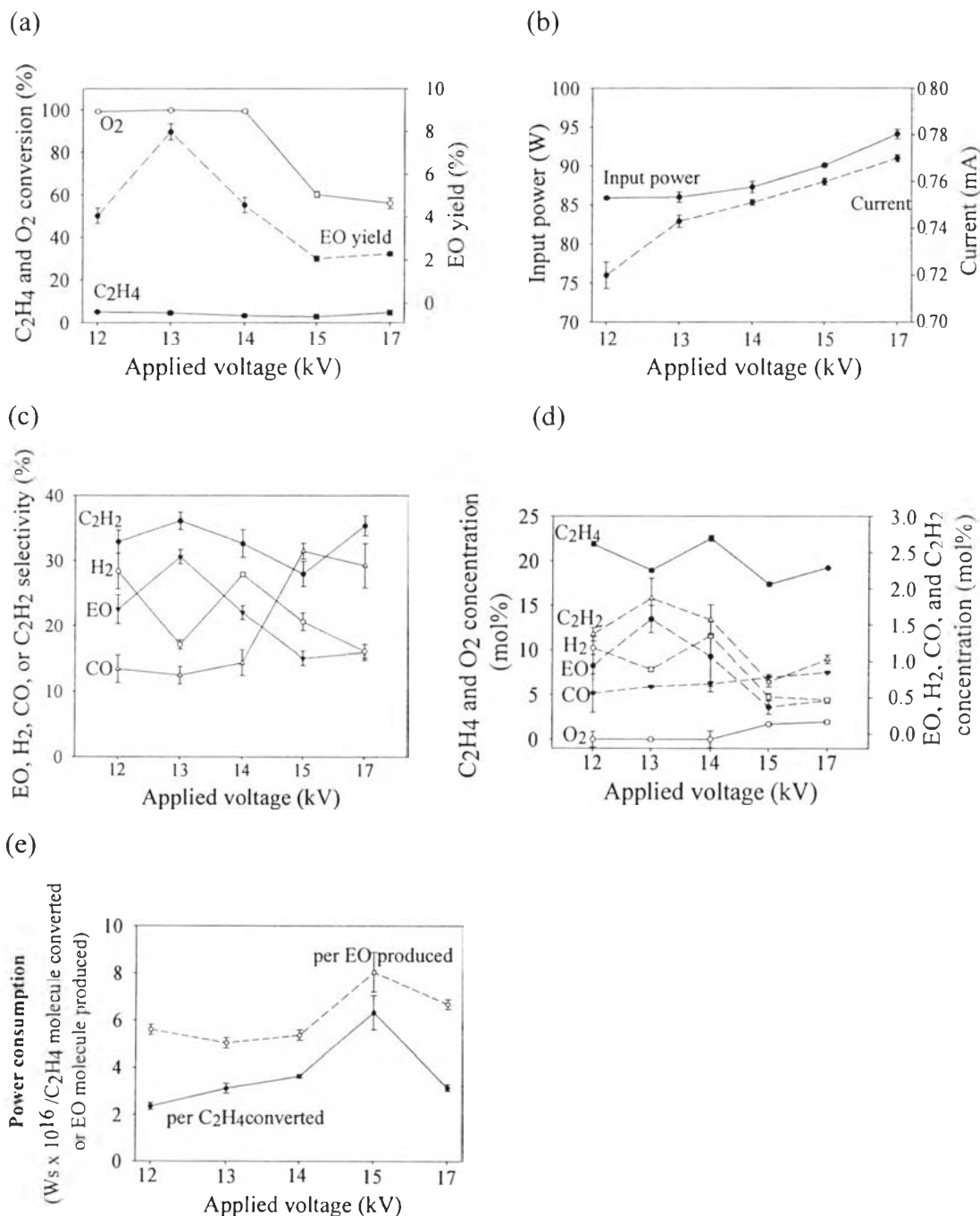


**Figure 5.4** (a) C<sub>2</sub>H<sub>4</sub> and O<sub>2</sub> conversions, and EO yield, (b) input power and current, (c) product selectivities, (d) outlet gas concentrations, and (e) power consumption as a function of applied voltage (a C<sub>2</sub>H<sub>4</sub> feed position of 0.25, an O<sub>2</sub>/C<sub>2</sub>H<sub>4</sub> feed molar ratio of 1/4, an input frequency of 500 Hz, and a total feed flow rate of 75 cm<sup>3</sup>/min).

with previous work [37,38] which showed an increase in  $O_2$  conversion with increasing applied voltage and generated current. This can be due to the fact that in the applied voltage range of 12–14 kV, the input power and generated current were sufficient to generate oxygen active species for the subsequent reactions including ethylene epoxidation, leading to a very high  $O_2$  conversion ( $\sim 100\%$ ). However, the  $O_2$  conversion significantly decreased when the system was operated at an applied voltage above 14 kV. The explanation is that an increase in excessive oxygen active species with increasing applied voltage results in increasing the recombination rate to form more oxygen molecules, leading to lowering  $O_2$  conversion with higher applied voltage under the separate  $C_2H_4/O_2$  feed condition.

As shown in Figure 5.4(c), the EO and  $C_2H_2$  selectivities increase when the applied voltage increases from 12 to 13 kV, and then decrease with further increasing applied voltage from 13 to 17 kV. In contrast to the EO selectivity, the CO selectivity remained almost constant at low applied voltages in the range of 12–14 kV, then sharply increased with increasing applied voltage in the range of 14–15 kV, and finally decreased slightly with further increasing applied voltage above 15 kV. Additionally, the  $H_2$  selectivity tended to decrease with increasing applied voltage and dropped to a minimum at the applied voltage of 13 kV. These results can be explained by the fact that with increasing applied voltage, the cylindrical DBD system produced more available electrons (Figure 5.4(b)); leading to increasing collision opportunities between the highly energetic electrons and both the  $C_2H_4$  and  $O_2$  reactants. Therefore, the EO selectivity increased with increasing applied voltage up to 13 kV. However, a larger amount of active species with an increase in applied voltage above 13 kV is more likely to promote combustion reactions instead, resulting in an enhancement of the CO selectivity and a reduction of the EO selectivity (Figure 5.4(c)).

Figure 4d illustrates the effect of applied voltage on the concentrations of  $C_2H_4$  and  $O_2$  remaining reactants, EO, and other main products, such as  $H_2$ , CO, and  $C_2H_2$ . With increasing applied voltage, the  $O_2$  concentration slightly increased while the  $C_2H_4$  concentration tended to remain almost unchanged in the range of 17–23%. Interestingly, the EO concentration had the same trend as the EO selectivity (Figure 5.4(c)) and EO yield (Figure 5.4(a)) in the way that they initially increased to

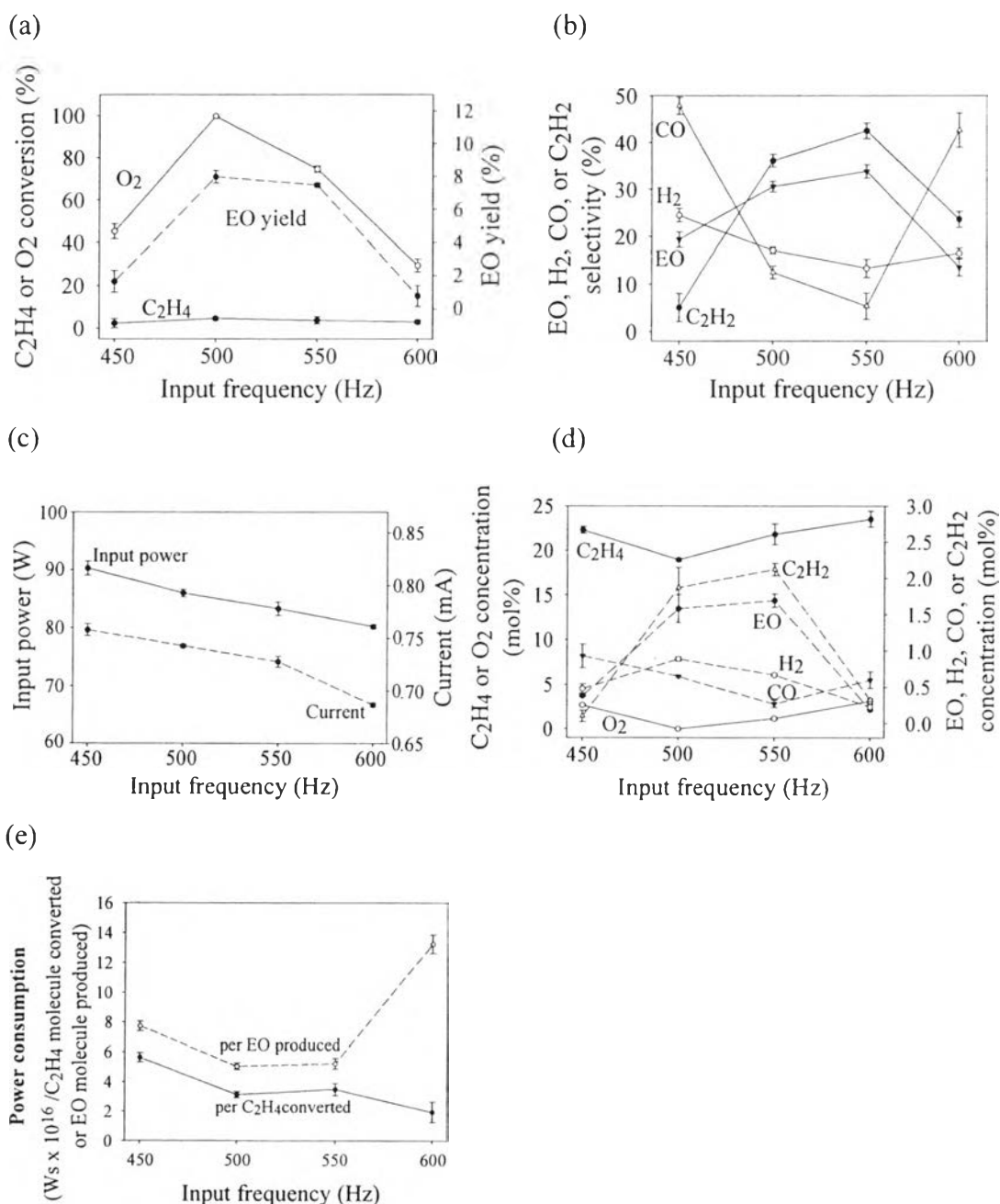
reach maximum values at an applied voltage of 13 kV, and then decreased with further increasing applied voltage beyond 13 kV. The CO concentration was found to be very low (less than 1%) and only slightly increased with increasing applied voltage over the entire studied range. These results indicate that an appropriate applied voltage is needed to maximize the ethylene epoxidation reaction rather than dehydrogenation and hydrocarbon combustion (partial oxidation).

Figure 5.4(e) shows the power consumption per  $C_2H_4$  molecule converted or per EO molecule produced as a function of applied voltage. The power consumption per  $C_2H_4$  molecule converted tended to significantly increase with increasing applied voltage from 12 to 15 kV. However, the power consumption per EO molecule produced slightly decreased with increasing applied voltage from 12 to 13 kV. Beyond the applied voltage of 13 kV, it slightly increased with increasing applied voltage in the range of 13 to 15 kV. The power consumption per  $C_2H_4$  molecule converted or per EO molecule produced decreased significantly with increasing applied voltage from 15 to 17 kV. From the above mentioned results, the applied voltage of 13 kV was considered to be an optimum value because it could provide maximum ethylene epoxidation performance in terms of the highest EO selectivity and yield with the lowest CO selectivity and the lowest power consumption per EO molecule produced. Hence, the applied voltage of 13 kV was selected for further investigation.

#### 5.4.5 Effect of Input Frequency

The input frequency, which also directly affects the field strength in the plasma zone, was subsequently investigated in the cylindrical DBD system under the following conditions: a  $C_2H_4$  feed position of 0.25, an  $O_2/C_2H_4$  feed molar ratio of 1/4, an applied voltage of 13 kV, and a total feed flow rate of  $75 \text{ cm}^3/\text{min}$ . The generated plasma discharges were found to be not uniform and not steady at an input frequency below 450 Hz, while they became extinct when the input frequency was higher than 600 Hz. Therefore, the input frequency was studied in the range of 450-600 Hz. Figure 5.5(a) illustrates the  $C_2H_4$  and  $O_2$  conversions and EO yield as a function of input frequency. It can be observed that the  $O_2$  conversion initially increased with increasing input frequency up to 500 Hz, and then significantly

decreased with further increasing input frequency from 500 to 600 Hz, whereas the  $C_2H_4$  conversion remained nearly unchanged over the entire input frequency range.



**Figure 5.5** (a)  $C_2H_4$  and  $O_2$  conversions, and EO yield, (b) product selectivities, (c) Input power and current, (d) outlet gas concentrations, and (e) power consumption as a function of input frequency (a  $C_2H_4$  feed position of 0.25, an  $O_2/C_2H_4$  feed molar ratio of 1/4, a, an applied voltage of 13 kV, and total feed flow rate of  $75 \text{ cm}^3/\text{min}$ ).

The EO yield rapidly increases with increasing input frequency from 450 to 500 Hz, then remains almost unchanged in the input frequency range of 500–550 Hz, and finally decreases with further increasing input frequency from 550 to 600 Hz.

As shown in Figure 5.5(b), the EO and C<sub>2</sub>H<sub>2</sub> selectivities significantly increase with an increase in the input frequency from 450 to 550 Hz, and adversely decrease with further increasing input frequency over 550 Hz. In contrast to the EO selectivity results, an increase in the input frequency from 450 to 550 Hz resulted in decreases in the H<sub>2</sub> and CO selectivities, while they increased with further increasing input frequency beyond 550 Hz. The EO and C<sub>2</sub>H<sub>2</sub> selectivities significantly decreased, but the CO selectivity increased with increasing input frequency from 550 to 600 Hz. A possible explanation is that increasing input frequency causes a decrease in the generated current and input power (Figure 5.5(c)), corresponding to the reduction of the number of electrons generated (weaker field strength). Therefore, it causes a decrease in the amount of active species for subsequential chemical reactions including the epoxidation reaction, resulting in decreasing EO selectivity, concentration, and yield as well as C<sub>2</sub>H<sub>2</sub> selectivity. However, the generated current seemed to be too energetic at the input frequency below 500 Hz, and it predominantly caused hydrocarbon combustion and dehydrogenation to favorably occur instead of ethylene epoxidation at a very high plasma discharge current, which could be observed from the dramatically increased CO and H<sub>2</sub> selectivities with decreasing input frequency from 500 to 450 Hz. The drastic decrease in O<sub>2</sub> conversion with decreasing input frequency from 500 to 450 Hz resulted from excessive coke formation on the electrode surface at the input frequency of 450 Hz as compared to 500 Hz.

In Figure 5.5(d), both the C<sub>2</sub>H<sub>4</sub> and O<sub>2</sub> concentrations had the same trend; they initially decreased with increasing input frequency from 450 to 500 Hz, and then gradually increased when the input frequency further increased from 500 to 600 Hz. The EO and C<sub>2</sub>H<sub>2</sub> concentrations corresponded well to their selectivities (Figure 5.5(b)), of which they increased to reach maximum values at 550 Hz. In contrast, the CO concentration gradually decreased with increasing input frequency from 450 to 550 Hz, and then adversely increased with further increasing input

frequency over 550 Hz. In contrast, the  $H_2$  concentration initially increased with an increase in input frequency from 450 to 500 Hz, and then decreased beyond 500 Hz.

Figure 5.5(e) shows the power consumption per  $C_2H_4$  molecule converted or per EO molecule produced as a function of input frequency. The power consumption per  $C_2H_4$  molecule converted or per EO molecule produced markedly decreased with increasing input frequency from 450 to 500 Hz, and then remained nearly unchanged. However, the power consumption per EO molecule produced finally increased rapidly with further increasing input frequency from 550 to 600 Hz, but the power consumption per  $C_2H_4$  molecule converted decreased. From the results, the highest ethylene epoxidation performance in terms of the maximum EO selectivity and comparatively high EO yield, with the minimum selectivities for other main products ( $H_2$  and CO) and the minimum power consumption per EO molecule produced, was obtained at an input frequency of 550 Hz.

As mentioned before, both the applied voltage and input frequency affect the input power. The input frequency had a higher influence on the input power (Figure 5.6) and current (Figure 5.5(c)) than the applied voltage (Figure 5.4(b)). The increasing applied voltage increased the input power and current while the increasing input frequency decreased the input power and current. Therefore, both applied voltage and input frequency had to be optimized in order to minimize the power consumption per EO molecule produced or per  $C_2H_4$  molecule converted.

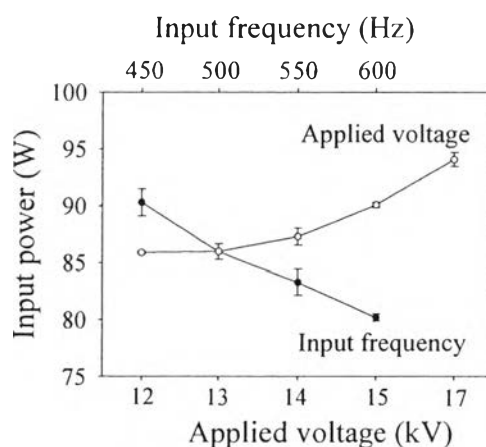


**Figure 5.6** Effect of input frequency and applied voltage on input power.

#### 5.4.6 Effect of Total Feed Flow Rate (or Residence Time)

To study the effect of total feed flow rate or residence time (total reactor working volume/total feed flow rate), the cylindrical DBD system was operated at different total feed flow rates of 60, 75, 100, and 125 cm<sup>3</sup>/min (Table 5.1), corresponding to residence times of 0.37, 0.29, 0.22, and 0.18 min, respectively. The total feed flow rate of 60 cm<sup>3</sup>/min was a minimum operationable flow rate due to the limitation of the electronic mass flow controllers. From the results shown in Figure 5.7(a), the C<sub>2</sub>H<sub>4</sub> conversion remains almost invariant over the entire total feed flow rate range while the O<sub>2</sub> conversion significantly increases with increasing total feed flow rate from 60 to 75 cm<sup>3</sup>/min, and then decreases drastically when the total feed flow rate further increases from 75 to 125 cm<sup>3</sup>/min. This is most likely due to the fact that an increase in the total feed flow rate, corresponding to a decrease in the residence time in the plasma zone, results in a shorter contact time for both the C<sub>2</sub>H<sub>4</sub> and O<sub>2</sub> molecules to collide with the generated electrons, leading to a decreasing O<sub>2</sub> conversion in the total feed flow rate range of 75 to 125 cm<sup>3</sup>/min. However, it is believed that the highly energetic oxygen active species easily recombine to the O<sub>2</sub> molecules rather than reacting with C<sub>2</sub>H<sub>4</sub> species to produce EO at the lowest total feed flow rate of 60 cm<sup>3</sup>/min (0.37 min); therefore, the O<sub>2</sub> conversion adversely decreased with decreasing total feed flow rate from 75 to 60 cm<sup>3</sup>/min. As shown in Figure 5.7(a), the EO yield increases rapidly to reach a maximum at a total feed flow rate of 75 cm<sup>3</sup>/min, and then decreases adversely with further increasing total feed flow rate over 75 cm<sup>3</sup>/min.

Figure 5.7(b) illustrates the effect of the total feed flow rate on the selectivities for EO (desired product), and other main products, such as H<sub>2</sub>, CO, and C<sub>2</sub>H<sub>2</sub>. The selectivities for CO<sub>2</sub>, CH<sub>4</sub>, and C<sub>3</sub>H<sub>8</sub> are not shown in this figure because they were extremely low (less than 3%). It can be seen that the EO selectivity mirrored the O<sub>2</sub> conversion in the way that the EO selectivity initially increased to reach a maximum at the total feed flow rate of 75 cm<sup>3</sup>/min, and then gradually decreased with further increasing total feed flow rate beyond 75 cm<sup>3</sup>/min. As a matter of fact, the oxygen active species react directly with the inactivated C<sub>2</sub>H<sub>4</sub>

molecules for EO formation. The CO selectivity was found to fluctuate over the entire total feed flow rate range, where its minimum was observed at a total feed flow rate of 75 cm<sup>3</sup>/min, corresponding to the maximum EO selectivity. The H<sub>2</sub> selectivity sharply decreased with increasing total feed flow rate from 60 to 100 cm<sup>3</sup>/min and there was no H<sub>2</sub> production at the total feed flow rate range from 100 to

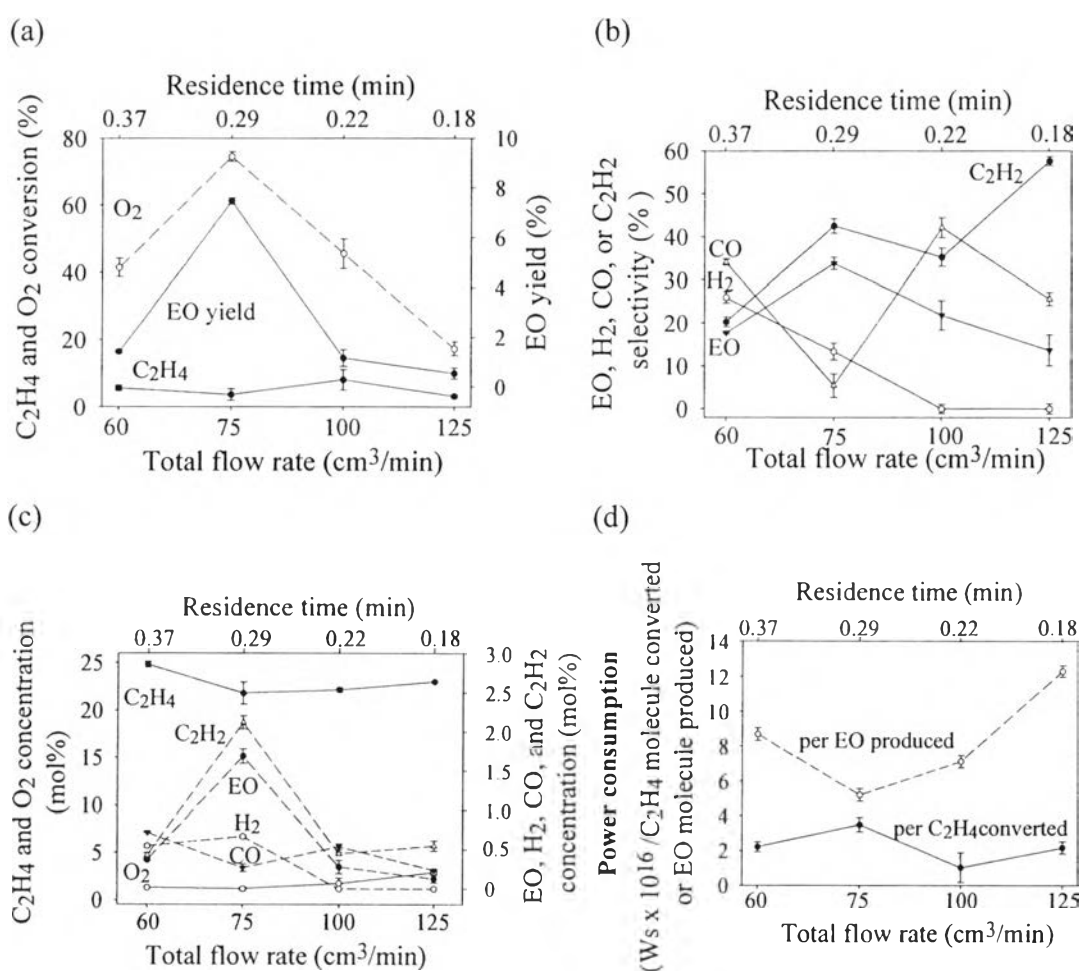


**Figure 5.7** (a) C<sub>2</sub>H<sub>4</sub> and O<sub>2</sub> conversions, and EO yield, (b) product selectivities, (c) outlet gas concentrations, and (d) power consumption as a function of total feed flow rate (a C<sub>2</sub>H<sub>4</sub> feed position of 0.25, an O<sub>2</sub>/C<sub>2</sub>H<sub>4</sub> feed molar ratio of 1/4, an applied voltage of 13 kV, and an input frequency of 550 Hz).

150 cm<sup>3</sup>/min. The C<sub>2</sub>H<sub>2</sub> selectivity tended to increase with increasing total feed flow rate. All the above mentioned results can be explained by the fact that an increase in

the total feed flow rate in the range of 75–125 cm<sup>3</sup>/min reduced the opportunity of collisions between electrons/oxygen molecules and oxygen active species/ethylene molecules, leading to a decrease in the ethylene epoxidation performance in terms of lower EO selectivity and yield. However, the results clearly reveal that hydrocarbon combustion, cracking, and further secondary reactions occurred instead of ethylene epoxidation when the collision opportunity was extremely high at the lowest total feed flow rate of 60 cm<sup>3</sup>/min (the longest residence time of 0.37 min), resulting in high CO and H<sub>2</sub> selectivities but low EO and C<sub>2</sub>H<sub>2</sub> selectivities.

From the results shown in Figure 5.7(c), the C<sub>2</sub>H<sub>4</sub> concentration, representing the remaining C<sub>2</sub>H<sub>4</sub> in the outlet gas, decreased slightly with increasing total feed flow rate up to 75 cm<sup>3</sup>/min, and then remained almost unchanged with further increasing feed flow rate in the range of 75–125 cm<sup>3</sup>/min, while the O<sub>2</sub> concentration increased slightly over the entire total feed flow rate range. The EO and C<sub>2</sub>H<sub>2</sub> concentrations greatly increased with increasing total feed flow rate until reaching maximum values at a total feed flow rate of 75 cm<sup>3</sup>/min, and then decreased adversely with further increasing total feed flow rate from 75 to 125 cm<sup>3</sup>/min. In contrast, the H<sub>2</sub> concentration remained almost invariant in the low total feed flow rate range of 60–75 cm<sup>3</sup>/min, and then decreased to zero level at high total feed flow rates in the range of 100–125 cm<sup>3</sup>/min. Even though the CO selectivity fluctuated slightly over the entire total feed flow rate range, it reached a minimum at a total feed flow rate of 75 cm<sup>3</sup>/min. As shown in Figure 5.7(d), the EO yield has the same trend as the EO selectivity and concentration; it increases rapidly to reach a maximum at a total feed flow rate of 75 cm<sup>3</sup>/min, and then decreases adversely with further increasing total feed flow rate over 75 cm<sup>3</sup>/min.

The power consumption per C<sub>2</sub>H<sub>4</sub> molecule converted or per EO molecule produced as a function of total feed flow rate is shown in Figure 5.7(e). An increase in the total feed flow rate did not significantly affect the power consumption per C<sub>2</sub>H<sub>4</sub> molecule converted, while the power consumption per EO molecule produced decreased moderately with increasing total feed flow rate from 60 to 75 cm<sup>3</sup>/min, and then increased adversely with further increasing total feed flow rate over 75 cm<sup>3</sup>/min. It can be clearly observed that the cylindrical DBD system

operated with the total feed flow rate of  $75 \text{ cm}^3/\text{min}$  provided the lowest power consumption per EO molecule produced.

From the overall results shown above, the highest ethylene epoxidation performance for the separate  $\text{C}_2\text{H}_4/\text{O}_2$  feed system was achieved under the following optimum operational conditions: a  $\text{C}_2\text{H}_4$  feed position of 0.25, an  $\text{O}_2/\text{C}_2\text{H}_4$  feed molar ratio of 1/4, an applied voltage of 13 kV, an input frequency of 550 Hz, and a total feed flow rate of  $75 \text{ cm}^3/\text{min}$ , exhibiting maximum EO selectivity and yield, as well as with the minimum power consumption per EO molecule produced, with the lowest CO selectivity and concentration.

#### 5.4.7 Performance Comparisons between Separate and Mixed Feeds of $\text{C}_2\text{H}_4$ and $\text{O}_2$

Figure 5.8 compares ethylene epoxidation performance of the cylindrical DBD system operated between the separate feed and the mixed feed of  $\text{C}_2\text{H}_4$  and  $\text{O}_2$  under their own optimum conditions. The optimum conditions for the mixed feed were obtained in our previous work [37]. The separate  $\text{C}_2\text{H}_4/\text{O}_2$  feed provided lower  $\text{C}_2\text{H}_4$  conversion but higher  $\text{O}_2$  conversion than the mixed feed system (Figure 5.8(a)). However, the  $\text{C}_2\text{H}_4$  and  $\text{O}_2$  conversions are not appropriate indicators in determining which system provided better ethylene epoxidation performance. The EO selectivity and yield, as well as the power consumption per  $\text{C}_2\text{H}_4$  molecule converted and per EO molecule produced are considered to be much more important parameters to evaluate the system performance. The separate feed system required lower power consumption per EO molecule produced as compared to the mixed feed system, but the results of the power consumption per  $\text{C}_2\text{H}_4$  molecule converted exhibited the opposite trend. Interestingly, the separate feed system significantly enhanced the ethylene epoxidation performance in terms of EO selectivity (33.9%) and yield (7.5%) while the mixed feed system provided EO selectivity of 8.9% and EO yield of 2.6% (Figure 5.8(b)). This is because the separate feed system can reduce not only the opportunity of cracking of both  $\text{C}_2\text{H}_4$  and produced hydrocarbons, including EO product to form lighter molecules but also reduce the opportunity of combustion and dehydrogenation reactions, resulting in

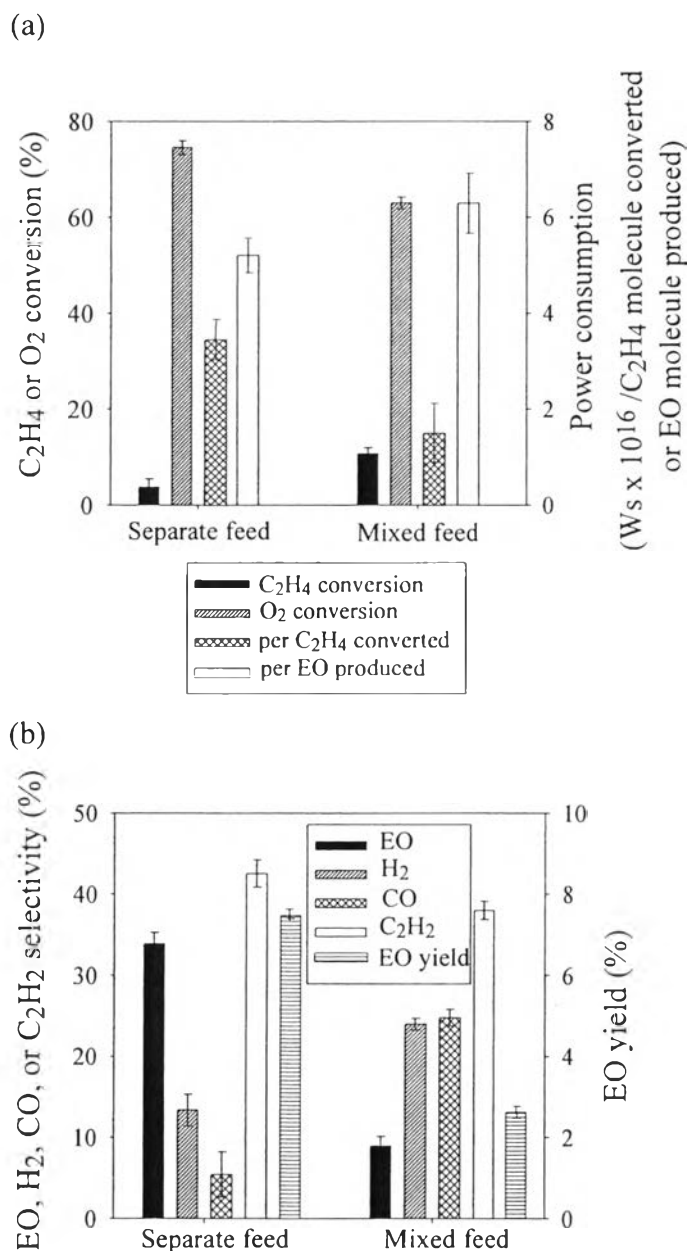


**Figure 5.8** Comparisons of the cylindrical DBD system performance using the separate C<sub>2</sub>H<sub>4</sub>/O<sub>2</sub> feed and the mixed C<sub>2</sub>H<sub>4</sub>/O<sub>2</sub> feed in terms of: (a) C<sub>2</sub>H<sub>4</sub> and O<sub>2</sub> conversions and power consumption and (b) main product selectivities and EO yield under their own optimum conditions [a C<sub>2</sub>H<sub>4</sub> feed position of 0.25 (for the separate feed), an O<sub>2</sub>/C<sub>2</sub>H<sub>4</sub> feed molar ratio of 1/4 (for both feed systems), an applied voltage of 13 kV (for the separate feed) and 15 kV (for the mixed feed), an input frequency of 550 Hz (for the separate feed) and 500 Hz (for the mixed feed), and a total feed flow rate of 75 cm<sup>3</sup>/min (for both feed systems)].

higher EO selectivity and yield with lower CO and H<sub>2</sub> selectivities as compared to the mixed feed system (even though the C<sub>2</sub>H<sub>2</sub> selectivity of the separate feed system was slightly higher).

For long-term stability testing, the studied DBD system was operated under optimum conditions for up to 36 h. Ethylene epoxidation activity was found to decrease gradually after 9 h. It is hypothesized that the thin layer of liquid product on the surfaces of the electrodes might be responsible for the drop in the process activity. Our future study will try to improve the EO selectivity and yield as well as long-term stability by applying a suitable catalyst with a stabilizer.

## 5.5 Conclusions

The separate C<sub>2</sub>H<sub>4</sub>/O<sub>2</sub> feed was, for the first time, applied for ethylene epoxidation in a cylindrical DBD system. The separate C<sub>2</sub>H<sub>4</sub>/O<sub>2</sub> feed and C<sub>2</sub>H<sub>4</sub> feed position were found to greatly influence the ethylene epoxidation performance. This is because the separate C<sub>2</sub>H<sub>4</sub> feed can reduce both of the reaction time between C<sub>2</sub>H<sub>4</sub> and activated O<sub>2</sub> and between C<sub>2</sub>H<sub>4</sub> and generated electrons. In addition, the separate C<sub>2</sub>H<sub>4</sub>/O<sub>2</sub> feed can reduce the residence time of C<sub>2</sub>H<sub>4</sub> molecules in the plasma region, depending on the C<sub>2</sub>H<sub>4</sub> feed position above the feed point of O<sub>2</sub>, leading to a reduction of all undesirable reactions of dehydrogenation, cracking, and coupling of C<sub>2</sub>H<sub>4</sub>, whereas the O<sub>2</sub> molecules are still mostly activated by the collision with the generated electrons. As a result, most of the inactivated C<sub>2</sub>H<sub>4</sub> molecules directly react with the oxygen active species to produce EO. However, if the C<sub>2</sub>H<sub>4</sub> feed position is too far away from the O<sub>2</sub> feed point, the reaction time between C<sub>2</sub>H<sub>4</sub> molecules (both activated and inactivated) and activated O<sub>2</sub> molecules is decreased, causing a negative effect to the ethylene epoxidation activity. Hence, the C<sub>2</sub>H<sub>4</sub> feed position of 0.25 is an optimum value for the maximum activity toward the ethylene epoxidation reaction.

## 5.6 Acknowledgements

The authors would like to gratefully acknowledge Dudsadeepipat Scholarship, Chulalongkorn University, Thailand, and Center of Excellence on Petrochemical and Materials Technology, Chulalongkorn University, Thailand.

## 5.7 References

1. Lefort TE (1931) Fr Patent FR 729952.
2. Campbell CT, Paffett MT (1984) *Appl Surf Sci* 19:28-42
3. Campbell CT (1986) *J Catal* 99:28-38
4. Tan SA, Grant RB, Lambert RM (1987) *Appl Catal* 31:159-177
5. Tan SA, Grant RB, Lambert RM (1987) *J Catal* 106:54-64
6. Rafael H, Arvind V, Enrico M (1990) *Stud Surf Sci Catal* 55:717-724
7. Jun Y, Jingfa D, Xiaohong Y, Shi Z (1992) *Appl Catal A: Gen* 92:73-80
8. Macieod N, Keel JM, Lambert RM (2003) *Catal Lett* 86:51-56
9. Jankowick JT, Barteau MA (2005) *J Catal* 236:379-386
10. Kapra AY, Orlik SN (2005) *Theoret Exp Chem* 41:377-381
11. Dellamorte JC, Lauterback J, Barteau MA (2007) *Ind Eng Chem Research* 48:5943-5953
12. Marta CN, Carvalho Ade, Passos FB, Schmal M (2007) *J Catal* 248:124-129
13. Rojluechi S, Chavadej S, Schwank JW, Meeyoo V (2007) *Catal Commun* 8:57-64
14. Torres D, Illas F, Lambert RM (2008) *J Catal* 260:380-383
15. Sreethawong T, Suwannabart T, Chavadej S (2009) *Chem Eng J* 115:396-403
16. Kim DB, Rhee JK, Moon SY, Choe W (2007) *Thin Solid Films* 515:4913-4917
17. Yu SJ, Chang MB (2001) *Plasma Chem Plasma Process* 21:311-327
18. Thevenet F, Couble J, Brandhorst M, Dubois JL, Puzenat E, Guillard C, Bianchi D (2010) *Plasma Chem Plasma Process* 30:489-502
19. Panorel I, Kornev I, Hatakka H, Preis S (2011) *Water Sci Technol: Water Supply* 11:238-345
20. Heintze M, Pietruszka B (2004) *Catal Today* 89:21-25

21. Li X, Bai M, Tao X, Shan S, Yin Y, Dai X (2010) *J Fuel Chem Technol* 38:195-200
22. Ouni F, Khacef A, Cormier JM (2009) *Plasma Chem Plasma Process* 29:119-130
23. Mora M, García MC, Jiménez-Sanchidrián C, Romero-Salguero FJ (2011) *Plasma Process Polym* 8:709-717
24. Nozaki T, Goujard V, Yuzawa S, Moriyama S, Agiral A, Okazaki K (2011) *J Phys D: Appl Phys* 44:art no 274010
25. Yu Q, Kong M, Liu T, Fei J, Zheng X (2011) *Catal Commun* 12:1318-1322
26. Rosacha LA, Anderson GK, Bechtold LA, Coogan JJ, Heck HG, Kang M, McCulla WH, Tennant RA, Wantuck PJ (1993) *Non-Thermal plasma Tech for Pollution Control, NATO ASI ser 34:Part B* 128-139
27. Durme JV, Dewulf J, Leys C, Langenhove HV (2008) *Appl Catal B: Environ* 78:324-333
28. Zhang Y, Li D, Wang H (2010) *Plasma Sci Technol* 12:702-707
29. Quoc Ana HT, Pham Huua T, Le Vana T, Cormierb JM, Khacefb A (2011) *Catal Today* 176:474-477
30. Suhr H, Schmid H, Pfeunds Schuh H, Iacocca D (1984) *Plasma Chem Plasma Process* 4:285-295
31. Torres G, Torres W, Prieto JA (2004) *Tetrahedron* 60:10245-10251
32. Suga Y, Sekiguchi H (2006) *Thin Solid Films* 506-507:427-431
33. Chavadej S, Kiatubolpaiboon W, Rangsunvigit P, Sreethawong T (2007) *J Mol Catal A: Chem* 263 128-136
34. Chavadej S, Tansuwan A, Sreethawong T (2008) *Plasma Chem Plasma Process* 28:643-662
35. Sreethawong T, Suwannabart T, Chavadej S (2008) *Plasma Chem Plasma Process* 28:629-642
36. Chernyak VYa, Olszewski SV, Yukhymenko VV, Solomenko EV, Prysiazhnevych IV, Naumov VV, Levko DS, Shchedrin AI, Ryabtsev AV, Demchina VP, Kudryavtsev VS, Martysh EV, Verovchuck MA (2008) *IEEE T Plasma Sci* 36:2933-2939
37. Sreethawong T, Permsin N, Suttikul T, Chavadej S (2010) *Plasma Chem Plasma Process* 30:503-524

38. Suttikul T, Sreethawong T, Sekiguchi H, Chavadej S (2011) Plasma Chem Plasma Process 31:273-290
39. Khani MR, Barzoki SHR, Yaghmaee MS, Hosseini SI, Shariat M, Shokri B, Fakhari AR, Nojavan S, Tabani H, Ghaedian M (2011) IEEE T Plasma Sci 39:1807-1813
40. Kline L, Partlow W, Bies W (1989) J Appl Phys 65:70-78
41. Coltrin ME, Dandy DS (1993) J Appl Phys 74:5803-5820
42. Yu B, Girschick S (1994) J Appl Phys 75:3914-3923
43. Ivanov V, Proshina O, Rakhimova T, Rakhimov A, Herrebout D, Bogaerts A (2002) J Appl Phys 91:6296-6302
44. Morrison N, William C, Milne W (2003) J Appl Phys 94:7031-7043
45. Farouk T, Farouk B, Gutsol A, Fridman A (2008) J Phys D: Appl Phys 41:art no 175202